

Observation of a comb of optical squeezing over many gigahertz of bandwidth

R.J. Senior¹, G.N. Milford², J. Janousek¹, A.E. Dunlop², K. Wagner¹,
H-A. Bachor¹, T.C. Ralph³, E.H. Huntington², and C.C. Harb²

¹Centre for Quantum-Atom Optics, Faculty of Science, The Australian National University,
Canberra, ACT, 0200 Australia

²Centre for Quantum Computer Technology, School of Information Technology and Electrical
Engineering, University College, The University of New South Wales, Canberra, ACT, 2600

³Centre for Quantum Computer Technology, Department of Physics, The University of
Queensland, St Lucia QLD 4072 Australia

C.Harb@adfa.edu.au

Abstract: We experimentally demonstrate the generation of optical squeezing at multiple longitudinal modes and transverse Hermite-Gauss modes of an optical parametric amplifier. We present measurements of approximately 3 dB squeezing at baseband, 1.7 GHz, 3.4 GHz and 5.1 GHz which correspond to the first, second and third resonances of the amplifier. We show that both the magnitude and the bandwidth of the squeezing at the higher longitudinal modes is greater than can be observed at baseband. The squeezing observed is the highest frequency squeezing reported to date.

© 2007 Optical Society of America

OCIS codes: (270.6570) Squeezed states; (040.5160) Photodetectors; (190.4970) Parametric oscillators and amplifiers.

References and links

1. N. Gisin, G. Ribordy, W. Tittel, and H. Zbinden, "Quantum cryptography," *Rev. Mod. Phys.* **74**, 145-195 (2002); F. Grosshans, G. Van Assche, J. Wenger, R. Brouri, N. J. Cerf, P. Grangier, "Quantum key distribution using gaussian-modulated coherent states," *Nature* **421**, 238-241 (2003).
2. C.M. Caves, "Quantum-mechanical noise in an interferometer," *Phys. Rev. D* **23**, 1693-1708 (1981).
3. B.J. Meers and K.A. Strain "Modulation, signal, and quantum noise in interferometers," *Phys. Rev. A* **44**, 4693-4703 (1991).
4. M. Nielsen and I. Chuang, *Quantum computation and quantum information*, (Cambridge University Press, Cambridge, UK, 2000).
5. R.W. Boyd, *Nonlinear Optics*, (Academic Press, 1992).
6. P.G. Kwiat, K. Mattle, H. Weinfurter, and A. Zeilinger, "New High-Intensity Source of Polarization-Entangled Photon Pairs," *Phys. Rev. Lett.* **75**, 4337-4341 (1995).
7. L.A. Wu, H.J. Kimble, J.L. Hall, and Huifa Wu, "Generation of Squeezed States by Parametric Down Conversion," *Phys. Rev. Lett.* **57**, 2520-2523 (1986).
8. Y. J. Lu and Z. Y. Ou, "Optical parametric oscillator far below threshold: Experiment versus theory," *Phys. Rev. A* **62** 033804 (2000).
9. C. Fabre and S. Reynaud, *Quantum noise in optical systems: A semiclassical approach*, J. Dalibard, J.M. Raimond and J. Zinn-Justin, eds. (Les Houches, Session LIII, 1990).
10. A.E. Dunlop, E.H. Huntington, C.C. Harb, and T.C. Ralph, "Generation of a frequency comb of squeezing in an optical parametric oscillator," *Phys. Rev. A* **73**, 013817 (2006).
11. G.N. Milford, C. C. Harb, and E. H. Huntington, "Shot noise limited, microwave bandwidth photodetector design," *Rev. Sci. Instrum.* **77**, 114701 (2006).
12. B. Yurke, P.G. Kaminsky, and R.E. Miller, "Observation of 4.2-K equilibrium-noise squeezing via a Josephson-parametric amplifier," *Phys. Rev. Lett.* **60**, 764-767 (1988).

13. R.W.P. Drever, J.L. Hall, F.V. Kowalski, J. Hough, G.M. Ford, A.J. Munley and H. Ward, "Laser phase and frequency stabilization using an optical resonator," *Appl. Phys. B* **B31**, 97-105 (1983).
14. "43 GBit/s DPSK Balanced Photoreceiver," http://www.u2t.de/pdf/Preliminary_Datasheet_BPRV2123_V10.pdf.
15. M.B. Gray, D.A. Shaddock, C.C. Harb, and H.-A. Bachor, "Photodetector designs for low-noise, broadband, and high-power applications," *Rev. Sci. Instrum.* **69**, 3755-3762 (1998).
16. G. Gonzalez, *Microwave Transistor Amplifiers: Analysis and Design*, 2nd Ed, (Prentice Hall, 1996).
17. Mini-Circuits, www.mini-circuits.com
18. M. G. Raymer, Jaewoo Noh, K. Banaszek and I. A. Walmsley, "Pure-state single-photon wave-packet generation by parametric down-conversion in a distributed microcavity," *Phys. Rev. A* **72** 023825 (2005).
19. D. F. Walls and G. J. Milburn, *Quantum Optics*, (Springer-Verlag, New York, 1994).
20. M. Lassen, V. Delaubert, C.C. Harb, P.K. Lam, N. Treps, H-A. Bachor, "Generation of squeezing in higher order Hermite-Gaussian modes with an optical parametric amplifier," *J. of the Euro Opt. Soc.-RP*, **1**, 06003 (2006).
21. K. McKenzie, N. Grosse, W.P. Bowen, S.E. Whitcomb, M.B. Gray, D.E. McClelland, and P.K. Lam, "Squeezing in the Audio Gravitational-Wave Detection Band," *Phys. Rev. Lett.* **93**, 161105 (2004).
22. H. Vahlbruch, S. Chelkowski, B. Hage, A. Franzen, K. Danzmann, and R. Schnabel, "Demonstration of a Squeezed-Light-Enhanced Power- and Signal-Recycled Michelson Interferometer," *Phys. Rev. Lett.* **95**, 211102 (2005).

1. Introduction

There have been numerous proposals for future technologies based on the unique properties of isolated quantum systems. These include quantum key distribution [1], ultra-high precision sensing [2, 3] and even quantum computers [4]. In real applications the functional specifications that emerge are low noise, high bandwidth and the ability to encode information into multiple degrees of freedom. Since quantum optics promises to meet these specifications, it is seen as a strong contender as the platform for a number of these quantum technologies.

Key resources required by quantum optical systems are non-classical states of light, which are commonly generated via non-linear optical processes. One such process is parametric down conversion (PDC), in which a high energy pump photon is converted into two lower energy photons, via a second order nonlinear interaction [5]. PDC is the underlying nonlinear process in optical parametric amplifiers (OPA), devices that are widely used in quantum optics experiments as sources of entangled photon pairs in discrete variable systems [6] and as sources of squeezing in continuous variable systems [7]. Entangled photon pairs exhibit stronger than classical correlations, and squeezed light exhibits noise fluctuations that are smaller than the quantum noise limit (QNL).

Cavity enhancement of PDC, which has been widely used to increase the strength of the non-linear process, leads to spectral filtering of the down converted output. Multimode behavior in cavity enhanced PDC has been observed in the discrete variable domain [8] and cavity enhancement has been identified in continuous variables since the early work of Wu *et. al.* [7]. Recent theoretical predictions have suggested that squeezed states should exist at all higher order longitudinal and transverse modes of a sub-threshold OPA [9, 10]. However until recently it was not possible to observe squeezing at the higher order longitudinal modes due to the limited bandwidth of sub-shot noise limited photodetectors. Advances in engineering design techniques for microwave photo-receivers have removed this limitation [11].

In this paper we report the first observation of squeezing spectra in four longitudinal cavity modes: baseband; 1.7 GHz; 3.4 GHz; and 5.1 GHz; and simultaneously two transverse modes: the TEM₀₀ and TEM₁₀ modes. Squeezing of microwaves has been observed in the very high frequency (VHF) band [12], however to the authors' knowledge we report here the widest optical squeezing bandwidth.

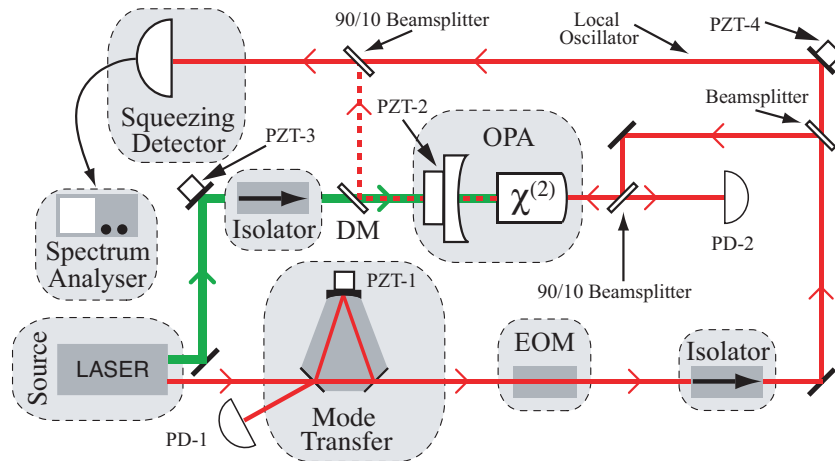


Fig. 1. Schematic of the experimental setup. Photodetector PD-1 detects the 12 MHz phase modulated signal emitted by the laser and generates an error signal which is sent to a mirror on a piezo-electric transducer PZT-1 to lock the mode transfer cavity (MTC). The electro-optic modulator (EOM) is used to impose 1 MHz and 16 MHz phase modulated signals on the transmitted MTC beam. These two signals are detected on PD-2 which then is used to derive error signals that are sent to PZT-2 and PZT-3 to lock the OPA cavity to the seed and to lock the OPA to de-amplification. The Pound-Drever-Hall locking technique [13] is used in all the locking loops. The local oscillator (LO) phase is swept using PZT-4 with respect to the phase of the squeezing to observe the amplitude and phase quadratures.

2. Experimental Setup

Squeezed light is produced using an OPA operating below threshold, see Fig. 1. The OPA is pumped with 532 nm light from a frequency-doubled diode-pumped Nd:YAG laser operating at 1064 nm. The OPA crystal has dimensions $2 \times 2.5 \times 6.5 \text{ mm}^3$ and is made from bulk LiNbO₃ which is 7% doped with MgO and phase-matched at 60°C. The OPA cavity is linear and is formed by the rear surface of the crystal (radius of curvature = 8 mm, high reflector at 532 nm, R=99.9% at 1064 nm) and an external mirror (radius of curvature = 75 mm, R=13% at 532 nm and R=96% at 1064 nm). The front surface of the crystal has a radius of curvature of 8 mm and is anti-reflection coated at both 1064 nm and 532 nm. The optical path length (OPL) of the OPA cavity is approximately 90 mm giving an FSR of 1.7 GHz.

The OPA is seeded with either a TEM₀₀ or TEM₁₀ mode at 1064 nm, with oscillation threshold at 200 mW and 350 mW pump power respectively. The system is operated as a de-amplifier with gains of 0.3 and 0.45 for the TEM₀₀ and TEM₁₀ modes respectively. Due to the fact that the system is operating in de-amplification mode lower gain values produce greater de-amplification. When operated as a squeezer, the OPA is seeded with 5 mW incident on the greater than 99.9% reflecting surface.

The spatial mode of the seed and the local oscillator determine which spatial mode of the squeezed beam will be observed and is controlled by a mode transfer cavity (MTC) (see Fig.1). The MTC can couple energy from the TEM₀₀ spatial mode of the incoming beam to higher order modes resonant in the cavity by misaligning the input beam. The output of the MTC is used to seed the OPA from the rear surface and as the local oscillator in subsequent measurements.

The squeezed light was detected on a single detector after being interfered with a strong local oscillator on a 90/10 beamsplitter, resulting in 90% of the squeezed light and 10% of the

local oscillator light reaching the detector.. The local oscillator power after the 90/10 beam-splitter was 7 mW for TEM₀₀, and 4.2 mW for TEM₁₀. The quantum noise level calibration was achieved by direct measurement of the local oscillator at the appropriate photocurrent.

This is a non-standard way to perform the measurements. There are two disadvantages to using this technique, the first being that the observable squeezing is reduced by the 10% lost at the beamsplitter and the second being that the noise floor of the measurement is set by the noise of the local oscillator. The latter is of no consequence here because the local oscillator is shot noise limited at microwave frequencies. Although this technique reduces the observed squeezing, the advantage is that it does not require a pair of balanced detectors and broadband subtracting circuitry as needed for homodyne detection. Improved levels of observed squeezing are expected with the future use of a balanced homodyne arrangement. Balanced receivers with appropriate bandwidth are available commercially for the telecommunications market (see for example [14]), however the sensitivity is not yet appropriate for the detection of squeezing.

Two different detectors were used to make the measurements. For baseband measurements, photodetectors have been developed in-house using lumped element design methods with readily available photodiodes and electronic components [15]. In particular, the baseband squeezing measurements were taken using a 500 μm diameter InGaAs photodiode with quantum efficiency of more than 95% using an AD829 amplifier in transimpedance mode. This detector had greater than 10 dB clearance between electronic noise and quantum noise from DC and 30 MHz. Note that the locking detectors for both the MTC and the OPA were of a lumped element design using 1 mm InGaAs photodiodes and LMH6624 amplifiers in transimpedance mode.

Higher bandwidth photodetectors require consideration of transmission-line effects that otherwise limit the utility of the lumped-element approach at microwave frequencies [16]. In [11] we describe such a photodetector that consists of a reverse-biased *pin* InGaAs photodiode, a microwave bandwidth amplifier and an inter-connecting matching network. This matching network achieves a broad-band power match between the AC shot noise power developed by the photodiode and the amplifier's 50 Ω input impedance. The photodetector is constructed as a microstrip circuit allowing close integration of the photodiode and associated bias circuitry, microstrip matching network and amplifier components (Mini-Circuits ERA MMIC [17]). Careful management of technical noise sources and circuit layout achieved a quantum efficiency of more than 92% and approximately 3 dB separation between electronic noise and quantum noise from 1.5 GHz to approximately 6 GHz, see [11] for more details.

3. Theory

A brief summary of the theoretical predictions for the outputs of the OPA is provided in this Section, more details may be found in references [9, 10]. Of interest here are the variances of the output amplitude and phase quadrature fluctuations normalized to the QNL as a function of Fourier frequency. The variance in the amplitude quadrature is denoted $V_{out}^+(\omega)$, and the variance in the phase quadrature is denoted $V_{out}^-(\omega)$ where ω is the Fourier frequency, i.e. the difference frequency between the optical carrier and the sidebands. The output variances are:

$$V_{out}^{\pm}(\omega) = \left| \frac{(\kappa \pm \chi)^2 - \left(\frac{1-e^{i\omega\tau}}{\tau}\right)^2}{\left(\kappa - \frac{1-e^{i\omega\tau}}{\tau}\right)^2 - \chi^2} \right|^2 V_{in}^{\pm}(\omega), \quad (1)$$

where the cavity decay rate is $\kappa = T/\tau$ and it is assumed to be set only by the transmission T of the output coupling mirror and the cavity round trip time τ . The nonlinear frequency conversion rate is χ and the down conversion bandwidth of the crystal is taken to be large compared to the Fourier frequencies of interest. The nonlinear frequency conversion rate is $\chi = 2\beta_{in}\chi^{(2)}$

where $\chi^{(2)}$ is the second order coefficient of nonlinearity for the nonlinear material and β_{in} is the amplitude of the pump field (assumed to be real without loss of generality). Equation 1 describes the frequency and phase dependent amplification (amplitude quadrature variance) or de-amplification (phase quadrature variance) of the noise of the seed. Minima in the squeezing spectrum are separated in frequency by the cavity free-spectral range (FSR) and occur at Fourier frequencies of $\omega = m\omega_{FSR} = 2\pi m/\tau$ for $m = 0, 1, 2, \dots$ within the downconversion bandwidth. Note that the resonance at $m = 0$ is the baseband squeezing spectrum. The downconversion bandwidth in a bulk nonlinear material of length L is estimated to be $10c/nL$ (c is the speed of light in vacuum, n is the refractive index of the material) [18]. Therefore, we estimate an upper bound of $m \approx 60$ for the crystals described herein.

The theory as it stands does not account for losses, which are modeled by a single beamsplitter placed after the OPA output using the standard beamsplitter equation [19]. The total loss in the system comprises terms due to:

- 1 intracavity loss of the OPA plus escape efficiency of output coupling, $(23 \pm 3)\%$;
- 2 optical losses between the OPA and the detection beamsplitter, $(6 \pm 1)\%$;
- 3 the quantum efficiency of the photodetector, worst case $(8 \pm 2)\%$;
- 4 non-ideal overlap of the local oscillator with the squeezed beam, $(7 \pm 2)\%$; and
- 5 loss of squeezing at the 90/10 detection beamsplitter, $(10 \pm 0.1)\%$.

The estimates indicated for each form of loss lead to a lower bound on the total system loss of $(54 \pm 4)\%$.

4. Experimental Results

Figures 2 and 3 show measurements of squeezing at baseband as well as the first, second and third FSRs of the OPA for both TEM₀₀ and TEM₁₀. On average the observed TEM₀₀ squeezing at baseband is approximately 2.5 dB and 3 dB at the higher resonances. Similarly, the observed TEM₁₀ squeezing at baseband is approximately 2 dB and 2.5 dB at the higher resonances. Note that the shape of the squeezing is dictated by the linewidth of the cavity and thus the profile of squeezing at higher FSRs is symmetric and the bandwidth is twice that of the baseband spectrum.

Overlaid on the upper traces of these figures are theoretical predictions of the output spectra of the OPA cavity assuming that the seed is quantum noise limited in both quadratures and at all frequencies. The theory curves were fitted to the measured results using: τ , which determines the frequency at which maximum squeezing is observed; χ , which determines the magnitude of squeezing; κ , which determines the width of the squeezing spectrum; and the total losses in the experiment, which determine the degree to which the squeezing is degraded and the anti-squeezing is attenuated. Table 1 shows the parameters used for each simulation.

Intuitively, one would expect that the magnitude of the squeezing should be identical at all resonances. This intuition arises from the expectation that de-amplification should be identical at each cavity resonance, which is indeed observed experimentally. However the input noise at baseband is very different to the input noise at higher frequencies and hence the output noise at baseband, which is simply de-amplified input noise, is very different to the output noise at higher frequencies. At low frequencies, laser noise and technical noise from the locking loops are dominant and act to corrupt the baseband squeezing. The large oscillations observed in the spectrum of the baseband measurements are from laser noise that is present from the

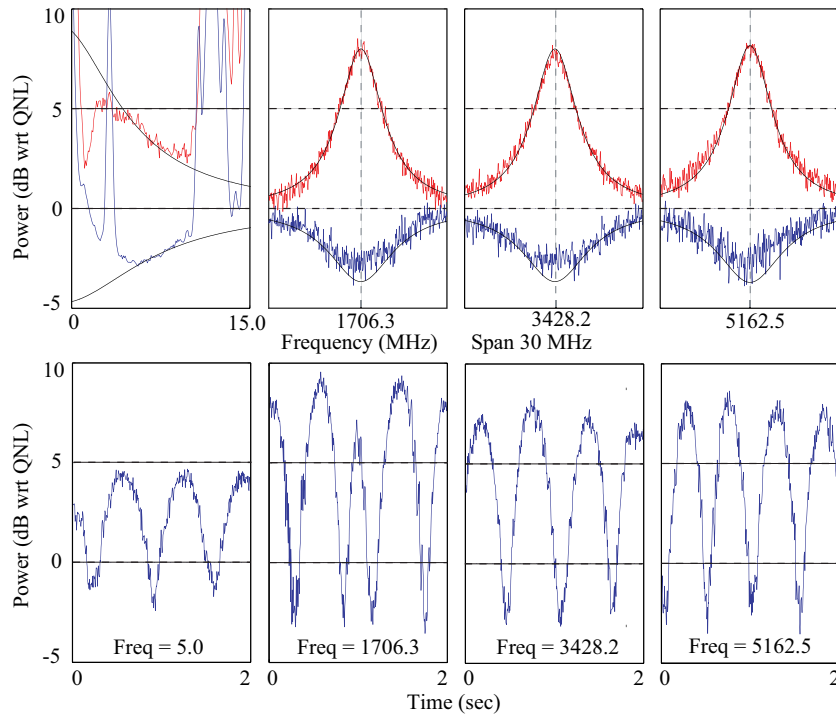


Fig. 2. TEM_{00} mode power spectrum of squeezing, normalised to the quantum noise limit. Upper traces show frequency measurements and theoretical predictions over a 15 MHz span at baseband, and 30 MHz span at the first, second and third FSRs; lower traces show zero span spectra as a function of sweeping the LO phase over a 2 second period. Zero span measurements are shown relative to the quantum noise level for the amplitude quadrature. The measurement resolution bandwidth is 1MHz and video bandwidth is 1 kHz for the high frequency results. Note that the baseband results show excess technical noise due to the imposed locking modulation signals.

Table 1. Parameters used to fit the theoretical simulations to the measured results.

Spatial Mode	Frequency	τ (GHz^{-1})	χ/κ	Losses
TEM_{00}	Baseband	0.5	0.32	47%
	1st FSR	0.586	0.32	57%
	2nd FSR	0.58337	0.32	57%
	3rd FSR	0.58111	0.325	57%
TEM_{10}	Baseband	0.55	0.17	45%
	1st FSR	0.5844	0.2	50%
	2nd FSR	0.58295	0.19	50%
	3rd FSR	0.58117	0.15	50%

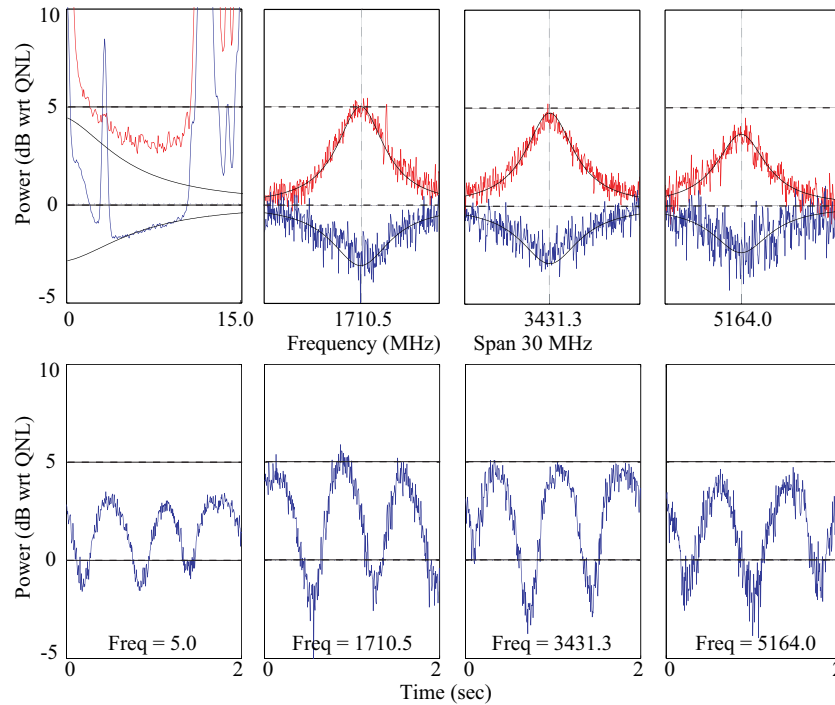


Fig. 3. TEM_{10} mode power spectrum of squeezing, normalised to the quantum noise limit. Upper traces show frequency measurements and theoretical predictions over a 15 MHz span at baseband, and 30 MHz span at the first, second and third FSRs; lower traces show zero span spectra as a function of sweeping the LO phase over a 2 second period. Zero span measurements are shown relative to the quantum noise level for the amplitude quadrature. The measurement resolution bandwidth is 1MHz and video bandwidth is 1 kHz for the high frequency results. Note that the baseband results show excess technical noise due to the imposed locking modulation signals.

modulations used to lock the seed light to the OPA cavity. The modulations occur at the imposed modulation frequencies as well as the intermodulation beat frequencies.

By contrast, the seed at the higher longitudinal modes is free of technical noise that is often present at baseband. It therefore follows that the squeezing is expected to be of the same magnitude at all higher resonances and stronger at higher resonances than at baseband. This is consistent with the observations and reinforced by noting the strong agreement between measurement and theory based on a QNL seed at higher resonances and the strong disagreement at baseband. Note that the presence of the seed field produce a squeezed output that is bright in comparison to the vacuum, whereas the squeezing at the higher free spectral ranges is not contaminated by the seed light and is truly a squeezed vacuum.

It is observed that there is less squeezing for the TEM_{10} mode than observed for the TEM_{00} . This is because the OPA is pumped with the second harmonic of the seed beam at 532 nm in the TEM_{00} spatial mode. This pumping scheme is optimal when generating a TEM_{00} squeezed beam but results in reduced squeezing in comparison to TEM_{10} . This effect is described in detail in Lassen *et. al.* [20] and accounted for in Eq. 1 by a reduction in the value of χ .

An interesting feature of our spectra is that the minima for the TEM_{00} (1706.3 MHz, 3428.2 MHz and 5162.5 MHz) and TEM_{10} (1710.5 MHz, 3431.3 MHz and 5164.0 MHz)

modes do not occur at the same frequencies, nor are successive minima separated by the same frequency spacing. The frequency of the first minimum of the TEM₀₀ mode implies that the OPL of the OPA cavity is 87.7 mm compared to 87.9 mm inferred from the first minimum of the TEM₁₀ mode. Each of the subsequent minima in the squeezing for the TEM₀₀ mode imply that the OPL of the cavity successively shortens by 300 μm. Differences in the inferred OPL are not insignificant compared to the total OPL of the cavity. This effect requires further investigation.

Baseband squeezing has been observed at very low frequencies at the cost of considerable technical effort [21, 22], leading to the potential to observe very low frequency signals with a squeezed noise floor. However, squeezing produced at higher FSR's can be observed without the requirement of eliminating very low frequency technical noise.

Acknowledgments - This work was supported by the Australian Research Council Centres of Excellence scheme.

5. Conclusion

In conclusion, we have shown the only reported measurement of squeezed light at microwave sideband frequencies. Such optical states might be used to produce 'multiplexed entanglement' for quantum communications applications. Moreover we have observed squeezing in higher-order transverse modes, which provides additional degrees of freedom for the quantum systems.